UNIVERSITY of SAN CARLOS
SCIENTIA • VIRTUS • DEVOTIO

Determination of Surface Energies and Relative Stabilities of the Different Surface Facets of Face-centered Palladium Through the DFT-Based Modelling

Mark Ryan Rosal Tripole

The in-depth study of surfaces has been of great importance throughout the scientific age by the simple virtue that the properties of the surface of a material differ from that of the bulk in terms of energetics. This understanding can shed light and give educated insights into natural phenomena at the interfaces of materials. DFT calculations performed to obtain the surface energies of the (001), (111), (110), and (211) facets of face-centered Pd showed that the (111) configuration has the lowest energy is the most stable given its close-packed nature. The trends in the results obtained are in good agreement with those found in literature.

1. Introduction

The study of surfaces has great application in a large variety of scientific fields, all of which fall under the main study that is surface science. This is essentially the study of phenomena that occur at the interface of two phases [1]. Covering phenomena both physical and chemical in nature, the field of surface science includes the subareas of surface physics and surface chemistry [2]. To put things into perspective, the surface of a material is the boundary at which the atoms that make up one material terminate and interface with the atoms of a new material, and generally there is quite a difference between the surface of a material and its bulk form [3]. Surface science is important in many critical processes, such as enzymatic reactions at biological interfaces found in cell walls and membranes, in electronics at the surfaces and interfaces of microchips used in computers, and the heterogeneous catalysts found in the catalytic converter used for cleaning emissions in automobile exhausts [4].

The current work focuses more on the study of the surfaces that can be derived from periodically structured crystals, with the intent of delving deeper into the possibilities that exist when it comes to adsorption studies, lending itself to topics such as heterogeneous catalysis and the elucidation of reaction mechanisms [5]. In order to do this, the concept of surfaces and interfaces must be understood, as well as the difference between the bulk material and surface material. Surfaces and interfaces define the boundary between a material and its surrounding environment, and so influence interactions with that environment. At the molecular level, the surface atoms have a different chemical environment, that is, fewer nearest neighbors, from that in the bulk. As a consequence, these surface atoms with changed atomic and electronic structures exhibit high chemical reactivity. This property makes surfaces and interfaces a favored medium for chemical and biological processes in nature and in technological applications [6].

With what was discussed in the previous paragraph, it can be seen the difference in reactivity between the bulk and a surface can be attributed to energetics, in that for the latter it is considered as the surface energy. At the surface of a material, there is a considerable amount of unbalanced interactions as compared to those in the bulk. As a result, surface energies, which arise from the unbalanced interactions mentioned previously, will be generally different from the bulk energy, though they do have a positive correlation with each other [7]. The high reactivity is simply a way for the surface to attempt to minimize its energy.

Surface energies are generally determined through what are known as contact angle experiments [8], which as of modern times are standardized and simple in that they are automated. Mathematical models are then applied to the results of these experiments to determine surface energy, all that stem from modifications of equations by Young and Dupré [9]. Of these, the most common is the Owens-Wendt-Rabel & Kaelble (OWRK) model given its linear nature, which is shown below:

$$\frac{\sigma_l(cos\theta+1)}{2\left(\sqrt{\sigma_l^D}\right)}=\left(\sqrt{\sigma_s^P}\right)\frac{\sqrt{\sigma_l^P}}{\sqrt{\sigma_l^D}}+\sqrt{\sigma_s^D}$$

Where σ_l and σ_s are the surface tension of the liquid and the surface energy of the solid, respectively, and the superscripts P and D are related to the polar and dispersive interactions, respectively, related to those parameters [10] [11]. θ denotes the contact angle of the liquids used during the experiment.

Over the development of computational modelling, the ease with which the simulation of the surfaces of

various materials can be done using computational packages has paved the way for more efficient DFT-based calculations for surface properties, mainly because it can simulate conditions that are ideal for the computation process. Ideally, the solid surface is created by cleaving the bulk material into two, thereby exposing the two surfaces, without any interference from any of the surrounding gas or liquid. That is, cleavage must occur in a perfect, ultra-high vacuum [12]. Computational modelling can simulate this perfectly, and the planes along which the cleavage can be done can be defined using Miller indices. Each unique configuration, or facet, that arises as a result of the cleavage along that particular plane will have its own unique surface energy, which is to be expected because there will be differences in the spatial distribution of the atoms on the surfaces of these facets. The actual computation for surface energy is done using the equation below:

$$\sigma_s = \frac{E_{slab} - nE_{bulk}}{2A}$$

Where: E_{slab} Total energy of facet/slab
E_{bulk} Energy of bulk material per atom
n Number of atoms in facet/slab
A Surface area of facet/slab

For the current work, computational simulation was done to create the different surface facets for face-centered Pd, namely the (001), (111), (110), and (211) configurations. DFT-based calculations were then performed to determine their respective surface energies, and inferences were made with regard to their stabilities relative to each other and relative to the bulk material. Computed values were then compared with experimental and other computationally obtained values by other researchers in scientific literature. The insights gained from the current study will be invaluable in the further study of surfaces for various applications, particularly into their potential and efficiency for catalysis and other specific reactions.

2. Results and Discussion

The computed values for the surface energies of the used surface facets of the face-centered Pd lattice are shown in Table 1, and graphical representations of the surface facets are shown in Figure 1 on the following page. As far as the values go, it can be seen that of all of the surface facets, the (111) configuration has the lowest surface energy, implying that for Pd this will be the most stable surface. This also gives insight into the similarity that this particular configuration has to the bulk structure of the Pd fcc lattice given its relative lower energy. And as stated in the previous section, the lower energy can be attributed to the spatial distribution of the atoms in the (111) configuration, which upon calculation of the planar density and packing fraction (1.480 x 10^{15} atoms/cm^2 and 0.9069, respectively) for this particular facet shows it to be close-packed structure. In comparison, the open (110) configuration actually has a packing fraction of 0.555, much smaller than that of the (111) packing fraction, which can also be directly related to its relative expected and computer surface energy. That is, the atoms in the open structure have more of these unbalanced interactions as a result of the cleaving, resulting in a higher surface energy when compared to the close-packed (111) facet. The (211) configuration has a significantly higher energy compared to the other facets, being the amalgamation of low index planes to form a vicinal or stepped surface, specifically composed of (111) terraces and (100) steps. Same as before, the increase in surface energy relative to surfaces cleaved from low index planes can be attributed to the spatial distribution of atoms in the surface. The vicinal structure actually provides a particular heterogeneity to the overall surface that has an effect on its energy and overall how it will react depending on its environment.

To visualize this clearly, reference can be made to the representations of the surfaces shown in Figure 1. These are useful in observing the spatial distribution of atoms across the surface as they are in the slab, more so for the close-packed (111) facet and the (211) vicinal or stepped

Table 1.
Calculated values for surface energies of the listed surface facets of face-centered Pd.

Surface Facet	E_{bulk} (eV)	E_{slab} (eV)	n	A (x 10^{-19} m^2)	σ (x 10^{18} eV/m^2)	σ (J/m^2)
(001)	-4504.391	-36032.436	8	1.560	8.631	1.38
(111)		-72065.887	16	2.702	8.091	1.30
(110)		-36031.029	8	2.217	9.291	1.49
(211)		-180161.265	40	7.644	9.410	1.51

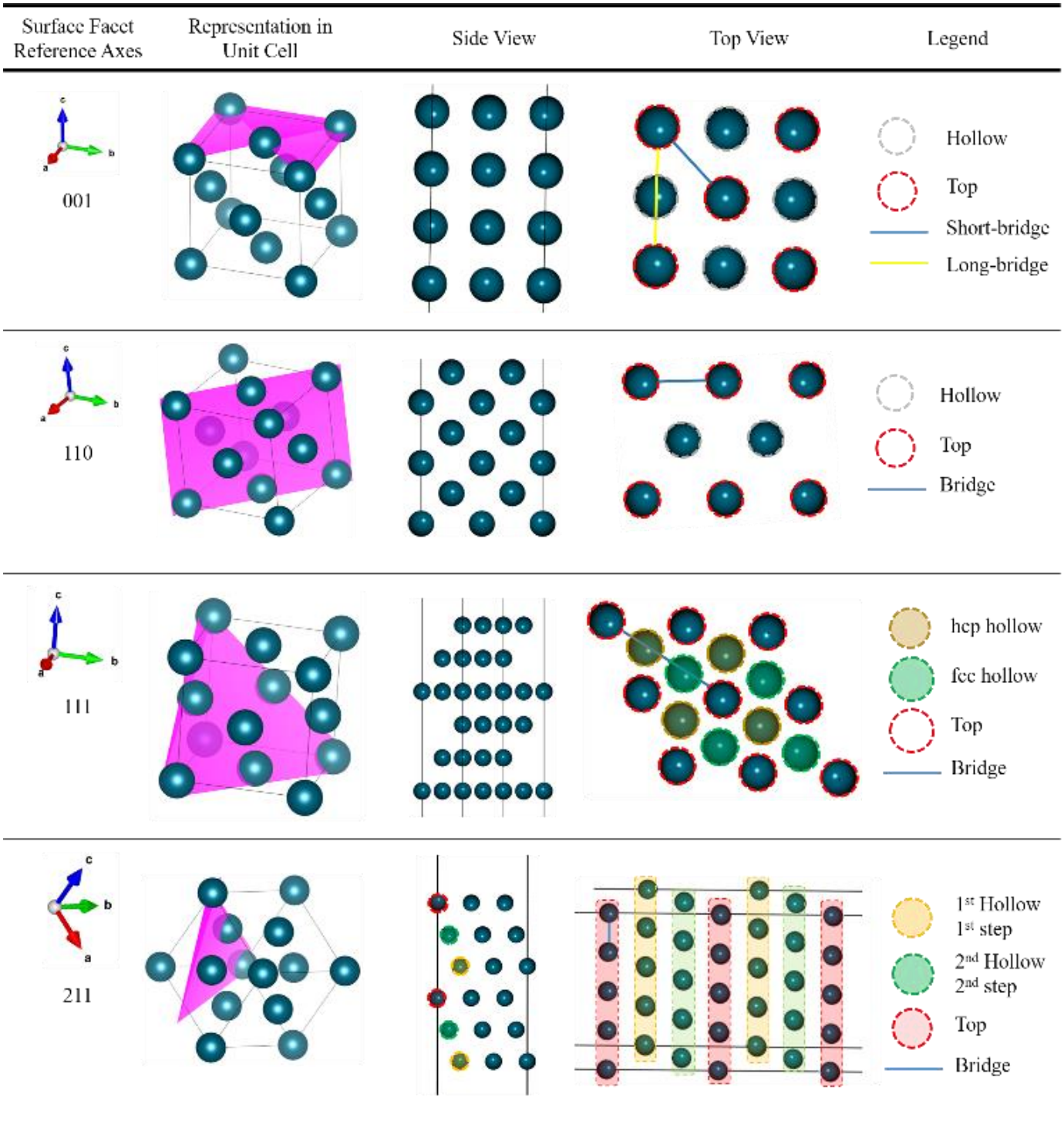

Figure 1. Graphical representations of the surface facets of face-centered Pd periodic lattice. The views of the surface from the side and from the top of the slab are shown for better visualization. The different sites of each surface facet are labeled according to the legend shown.

surface. The packed nature of the (111) surface facet can be clearly seen, with the central atom of the top layer being surrounded by 6 atoms as its nearest neighbors and three in the layer immediately below to satisfy a coordination number of 9. For the (211) surface facet, the three-atom wide terrace can be seen (more clear from the side view, highlighted in orange, green and red), which implies that the stepped portion is the drop after the atom layer on the top that is labelled in red. For the (110) surface, the top view shows the open structured nature of the slab, showing a significant hollow layer between the two top most atom layers, which is numerically supported by its lower packing fraction compared to the (111) surface facet as mentioned in the previous paragraphs. To further validate the calculations made in the current study, comparisons

were also made to the results obtained by other researchers in the field, and these are tabulated in Table 2.

Table 2.
Calculated values from the current work shown along with literature values obtained from various researchers ([13] – [19]).

Surface Facet	Computed σ (J/m^2)	Literature Values (J/m^2)
(001)	1.38	2.172 [13] 2.326 [14]
(110)	1.49	2.311 [13] 2.225 [14] 1.490 [15] 1.570 [16] 1.671 [17]
(111)	1.30	1.890 [13] 1.920 [14] 1.220 [15] 1.360 [16] 1.382 [17] Experimental 2.00 [18] 2.03 [19]
(211)	1.51	2.430 [13] 2.347 [14] 1.410 [15] 1.610 [16] 1.617 [17]

As can be seen in Table 2, there is a relatively high of agreement between the values obtained in the current work to those that have been obtained by other researchers. Though there may be differences in the values themselves to a certain degree due to the differences in the conditions imposed and computational models used, the most striking agreement comes in the fact that the (111) surface facet is the most stable surface for face-centered Pd. The trends in the values themselves are almost the same, save for the results from [15] which show the (211) surface facet to be more stable compared to the (111) configuration.

3. Conclusion

DFT-based calculations for the surface energies of the (001), (110), (111), and (211) surface configurations of face-centered Pd show that the (111) facet is the most stable surface by virtue of its lower surface energy. This can be attributed to the spatial distribution of atoms in the close-packed structure, having a higher packing fraction compared to the other lower index plane facets. The results obtained are in good agreement with literature values, and this goes to show the degree of accuracy that can be obtained in predictive studies using computational modelling of surfaces. This will be invaluable in delving deeper into the potential of surfaces in view of a whole slew of applications, both in physics and in chemistry.

Computational Model

Spatial representations of surface facets were obtained through modelling in VESTA (Visualization for Electronic and Structural Analysis). DFT calculations were implemented using Quantum Espresso with exchange-correlation term described using the generalized gradient approximation (GGA) based on Perdew-Burke-Ernzerhof (PBE) functional. The interaction between ions and electrons were described using the projector augmented wave (PAW) method. Plane wave basis sets were employed with an energy cut-off of 400 eV. The surface Brillouin zone integrations were performed on a grid of 4 x 4 x 1 Monkhorst-Pack k-points using Methfessel-Paxton smearing of $\sigma = 0.2$ eV.

Notes and References

[1] Luklema, J.; 1995–2005, Fundamentals of Interface and Colloid Science. 1–5. Academic Press.
[2] Prutton, M; 1994, Introduction to Surface Physics. Oxford University Press. ISBN 978-0-19-853476-1.
[3] Somorjai, G.A.; 1995, Introduction to Surface Chemistry. New York: Academic Press.
[4] Zangwill, A.; 1988, Physics at Surfaces. Cambridge, UK: Cambridge University Press.
[5] Fischer-Wolfarth, J. et al.; 2010, "Particle-size dependent heats of adsorption of CO on supported Pd nanoparticles as measured with a single-crystal microcalorimeter". Physical Review B. 81 (24): 241416.
[6] Somorjai GA, Li Y; 2010, Introduction to Surface Chemistry and Catalysis (Wiley, Hoboken, NJ), 2nd Ed.
[7] Fowkes, F.M.; 1964, Attractive Forces At Interfaces, Ind. Eng. Chem. (56), 40–52
[8] Marshall, S.J. et al.; 2010, "A review of adhesion science". Dental Materials. 26 (2): e11–e16
[9] "Surface Free Energy: Measurements". biolinscientific.com. Biolin Scientific. Retrieved April 11, 2020
[10] D.K. Owens et al.; 1969, Estimation of the surface free energy of polymers, , J. Appl. Polym. Sci. (13), 1741–1747
[11] D.H. Kaelble, Adhes, J.; 1970, Dispersion-Polar Surface Tension Properties of Organic Solids, 66–81
[12] Kasemo, B.; 2017, Surface Science – How it all began, from an experimental perspective, Biolin Scientific, Surface Science Blog. Retrieved April 11, 2020
[13] Fu, B., Liu, W., Li, Z.; 2010, Calculation of the surface energy of fcc-metals with the empirical electron surface model, Applied Surface Science 256 (2010) 6899-6907
[14] L., Vitos, A.V. Ruban, H.L. Skriver, J. Kollar, Surf. Sci. 411 (1998) 186.
[15] Yan-Ni Wen, Jian-Min Zhang, Surface Energy Calculation of the fcc metals by using the MAEAM, Solid State Communications 144 (2007) 163 - 167
[16] Calculations from Materials Project. Retrieved April 11, 2020
[17] Zhang, J.M., Ma, F., Xu, K.W.; 2004, Calculation of the surface energy of FCC metals with modified embedded-atom method Applied Surface Science 229 34–42
[18] Patraa, A. et al.; 2017, Properties of real metallic surfaces: Effects of density functional semilocality and van der Waals nonlocality, PNAS Early Edition
[19] Sansa, M., Douib, A., Guesmi, H.; 2014, Density functional theory study of CO-induced segregation in gold-based alloys, The Journal of Chemical Physics 141, 064709 (2014);